Int. J. Electrochem. Sci., 9 **(2014)** 1399 - 1414

International Journal of
ELECTROCHEMICAL
SCIENCE
www.electrochemsci.org

A Novel Label-Free Amperometric Immunosensor Based on Graphene Sheets-Methylene Blue Nanocomposite/Gold Nanoparticles

Lu Qiao, Xiangyou Wang[*]*, Xia Sun*[*]

School of Agriculture and Food Engineering, Shandong University of Technology, NO.12, Zhangzhou Road, Zibo 255049, Shandong Province, P.R. China
[*]E-mail: wxy@sdut.edu.cn; sunxia2151@sina.com

Received: 18 July 2013 / *Accepted:* 19 November 2013 / *Published:* 5 January 2014

In this study, a sensitive, label-free amperometric immunosensor based on graphene sheets-methylene blue nanocomposite and gold nanoparticles (GS-MB/GNPs) for the direct determination of chlorpyrifos residues was exploited. To fabricate the immunosensor, GS was first dispersed with chitosan(CS) to obtain a homogeneous solution and then mixed with MB in a ratio of 2:1. The nanocomposite film of GS-MB was dropped on the surface of glassy carbon electrode (GCE) which was first modified by the electrodeposition of GNPs. The stepwise assembly process of electroactive species on electrode surface and the performance of the immunosensor was characterized by means of cyclic voltammetry (CV), electrochemical impedance spectroscopy (EIS) and scanning electron microscopy (SEM), respectively. The GS-MB nanocomposite possesses good electrochemical behavior and high binding affinity to the electrode. Furthermore, high surface areas of GS and vast aminos and hydroxyls of CS provide a platform for the crosslinking of antibody. Under optimal conditions, the proposed immunosensor showed a wide linear range from 1 to 500 ng/mL with a detection limit of 0.056ng/mL.The constructed immunosensor exhibited good reproducibility, high specificity, acceptable stability and regeneration performance, which provided a new promising tool for the detection of chlorpyrifos in real samples.

Keywords: amperometric immunosensor; gold nanoparticles; graphene sheets-methylene blue nanocomposite; chlorpyrifos.

1. INTRODUCTION

Chlorpyrifos (O,O-diethyl-O- (3, 5, 6-trichloro-2-pyridyl)-phosphorothioate), a broad spectrum OP insecticide, is one of the most widely used organophosphate insecticides in agriculture to control

pests and enhance production [1-3]. However, its persistence, bioaccumulation, and toxicity pose a potential hazard to human health and lead to extensive pollutions of the environment [4-6]. Therefore, for the sake of human health and environmental pollution control, the rapid and accurate determination of pesticide residues is of crucial importance, especially in field of on-line applications. The traditional analytical methods for chlorpyrifos detection involving gas chromatography (GC), high performance liquid chromatography (HPLC), capillary electrophoresis (CE) and mass spectrometry (MS) are sensitive, reliable and standardized techniques [7-9], but these methods require expensive instruments, skilled analysts and involve extensive time consumption and complicated pretreatment procedure [10-11].

It has been reported that biosensor measurements are a good method for the rapid detection of pesticide residues, because of their simple fabrication, easy operation, rapid response and high sensitivity [12]. Immunosensors are biosensors that are provided with the selectivity in view of immunological interactions and also being proposed and proved to be efficient analytical devices for the monitoring of organic pollutants in food and the environment [13-14]. The immobilization of biomolecules on the electrode is the most important factor in improving the performance of the immunosensors. In recent years, nano-materials have attracted widespread attention and been introduced to immunosensor to enhance the sensitivity of the electrochemical detection for targets [15, 16], such as metal nanoparticles [17], multiwall carbon nanotubes (MWCNTs) [18, 19], graphene sheets(GS) [20] and so on. Gold nanoparticles (GNPs) have been widely used for immobilization of biomolecules due to their large specific surface area, high electron-transfer ability and biocompatibility [21]. Chitosan (CS) is a biological cationic macromolecule containing large groups of amines and hydroxyls. It has been widely used for dispersion because of its good biocompatibility and film-forming ability [22, 23]. Recently, GS, a novel one-atom-thick and two-dimensional graphitic carbon system, has attracted great interests in various fields, including nanoelectronics, sensors, nanocomposites, and energy storage and conversion [17] since its discovery by Geim and cowork-ers in 2004 [24] . GS has the characteristics including large specific surface area, remarkable mechanical stiffness, high elasticity and excellent conductivity [20, 25-27]. Nevertheless, the water solubility of GS limits their further application in fabricating biosensors because GS is hydrophobic and tends to form agglomerates in water [28, 29]. Thus, CS was used as disperser to prepare homogeneous GS solution. Methylene blue (MB), a cationic dye, has well-known electrochemical properties in the solution phase. The electrochemical behavior of its monomer in conductive substrate is good and it has been used as a redox indicator [30-32]. However, such low molecular weight soluble mediator has disadvantageous that it can leach out of the electrode, which may lead to a significant signal loss and affect the stability of biosensor. And it is readily polymerized in electrolytes of phosphate-buffered solution (PBS). In order to overcome these defects, we have developed a new kind of nanocomposite material composed of GS and MB.

In this study, we aimed to improve the stability and maintain the activity of antibodies to develop a simple, stable and sensitive amperometric immunosensor. GS-MB nanocomposite, possessing good electrochemical behavior, was employed to immobilize antibody fragments on the sensor substrate surface without decreasing their binding affinities and binding capacities [27]. Furthermore, CS, served as dispersant, not only provide more amino groups to bond antibody but also

increase the stability of the GS-MB nanocomposite film immobilized onto the electrode surface. To the best of our knowledge, the kind of immunosensor based on GS-MB/GNPs has not been reported. The experimental conditions involving the proportion of GS-MB, the concentration of antibody, pH of the detection solution, incubation time and incubation temperature were investigated in detail. As a result, the obtained electrochemical immunsensor for the direct determination of chlorpyrifos exhibited excellent characteristics including high sensitivity, low detection limit and long-term stability.

2. MATERIALS AND METHODS

2.1 Reagents

Anti-chlorpyrifos monoclonal antibody and chlorpyrifos were both purchased from Lifeholder. Gold chloride ($HAuCl_4$) was obtained from Shanghai Sinopharm Chemical Reagent Co. Ltd. (China). GS were obtained from Nanoon Co., Ltd. (Beijing, China). Methylene blue (MB) was purchased from Tianjin Kemiou Chemical Reagent Co., Ltd. And glutaraldehyde solution(GA) was obtained from Sigma-Aldrich. Bovine serum albumin (BSA) was from BioDev-Tech. Co. Ltd. 0.01 M Phosphate buffer solution (PBS, pH 7.4, high-pressure sterilization) was used for dissolving the anti-chlorpyrifos monoclonal antibody. A PBS (0.1 M, pH 7.5) containing 5 mM $[Fe(CN)_6]^{3-/4-}$ and 0.1 M KCl was used as the detection solution. CHIT (95% deacetylation), ethanol and other reagents were of analytical grade and distilled water was used throughout the experiments.

2.2 Apparatus

Cyclic voltammetry (CV) and electrochemical impedance spectroscopy (EIS) and measurements were performed with CHI660D electrochemical workstation (Shanghai Chenhua Co., China). A conventional three-electrode system was employed with a saturated calomel electrode (SCE) as the reference electrode, a platinum electrode as the auxiliary electrode, and a glassy carbon electrode (GCE) (d=3 mm) or modified GCE as the working electrode. The morphologies of GNPs and GS-MB nanocomposites and the fabrication process of the immunosensor were observed by a scanning electron microscope (SEM, SIRION, FEI, Netherlands).

2.3 Preparation of the immunosensor

2.3.1 Preparation of GS-MB nanocomposites

50 mg chitosan flakes were weighed and dissolved in aqueous solution of 10 mL 1.0 wt.% acetic aced with magnetic stirring for about 3 h, and then the pH of the solution was adjusted to 4.0~5.0 with a concentrated NaOH solution. Subsequently, 10 mg GS was added into above 0.5 wt% CS and the solution should be ultrasonically dispersed for 6 h to give a stable black suspension.

1mg/mL MB solution was prepared by dissolving MB powder in ethanol solution. Then GS and MB were mixed together in different proportion.

2.3.2 Electrode surface cleaning

GCE (with a diameter of 3 mm) were sonicated in a mixture solution of "piranha solution" (H_2SO_4:30% H_2O_2 = 3:1) and rinsed with distilled water. The bare GCE was polished carefully with 0.3 and 0.05 μm alumina powder, respectively. Then they were immerged in 6.0 M HNO_3, absolute ethanol and distilled water in sequence for an ultrasonic bath for 5 min. Before modification, the bare GCE was scanned in 0.5 M H_2SO_4 between -1 and 1 V with a scan rate of 0.1 V/s until a steady-state curve was obtained. Then the electrode was rinsed with distilled water, and dried in air.

2.3.3 The fabrication of immunosensor

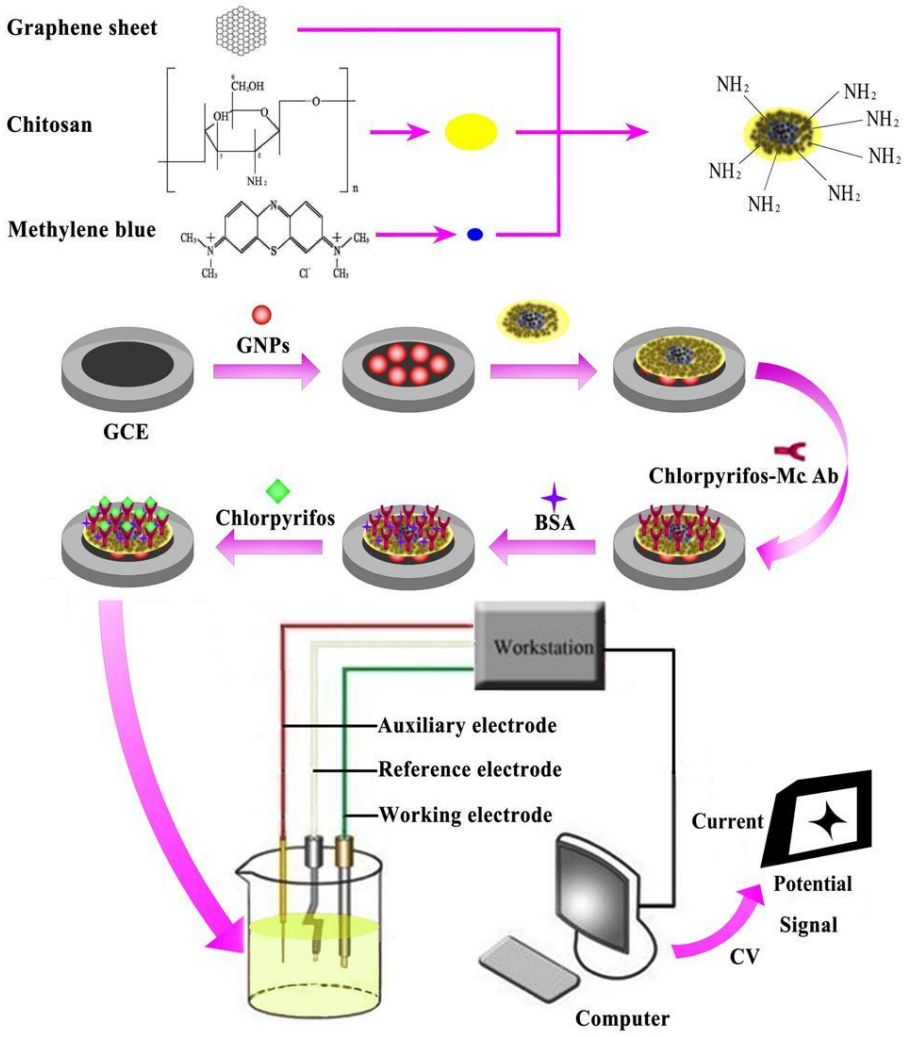

Scheme 1. Schematic illustration of the stepwise immunosensor fabrication process.

The cleaned GCE was treated with electrodeposition performed with current-time curve scaning at potential of -0.2V for 200s in 3 mM $HAuCl_4$ (denoted as GNPs/GCE). Then different proportions of homogeneous GS-MB nanocomposite were dropped onto the electrode surface (denoted as GS-MB/GNPs/GCE). To immobilize the antibody onto electrode interface, at first, the modified electrode was immersed in 5 % GA solution for 30 min in a shady environment. Afterwards the electrode was washed with distilled water to eliminate glutaraldehyde from the surface. Subsquently, the electrode was immersed in 200 ng/mL anti-chlorpyrifos antibody solution at 4°C for about 12 h (denoted as anti-chlorpyrifos/GS-MB/GNPs/GCE), thus the free amino groups on the antibody can be randomly coupled with several reactive moieties on the immunosensor substrate surface through the covalent cross-linking method. Then the multilayer modified electrode was incubated with 0.5% BSA (denoted as BSA/anti-chlorpyrifos/GS-MB/GNPs/GCE) at room temperature for 1 h in order to block nonspecific binding sites, and the electrode was rinsed with distilled water to remove the redundant amount of BSA. Finally, the resulted immunosensor was stored above the 0.1 M PBS at 4°C when not in use. The stepwise fabrication procedures of immunosensor was shown in Scheme 1.

2.4 Electrochemical measurements

The scanning electron micrographs of GNPs and GS-MB nanocomposite film were observed with SEM. All electrochemical measurements were performed in 10 mL of 0.1 M PBS (pH 7.5) containing 5 mM $K_3[Fe(CN)_6]/K_4[Fe(CN)_6]$ (1:1 mixture as a redox probe) and 0.1 M KCl at room temperature. Cyclic voltammetric (CV) measurements were performed over a potential range from -0.3 to 0.7 V at a scan rate of 50 mV/s (vs. SCE) in the above mentioned detection solution (pH 7.5). The impedance spectra was measured at a potential of 0.2 V in the frequency range from 0.1 to 10^5 Hz with a voltage amplitude of 5 mV. The chlorpyrifos detection was based on relative change in current response ($\%\Delta I = (I_0 - I_1)/I_0 \times 100\%$), where I_0 was the cathodic peak current of the CV after blocking nonspecific binging sites by BSA and I_1 was the cathodic peak current of the CV after immunoreaction to the chlorpyrifos.

2.5 Preparation and determination of real samples

Vegetable samples (cabbage, pakchoi, lettuce and leek) for detection study were purchased from the local supermarket and cleaned thoroughly using distilled water. Then the samples were dried in the air and chopped into 3×3 mm particles approximately. Different concentrations of chlorpyrifos solution were sprinkled on their surfaces. After equilibration for 3 h at room temperature to allow pesticide absorption onto the samples, a mixture of 1 mL acetone and 9 mL 0.1M phosphate buffer (pH 7.4) was added to each sample weighing 10 g. And then the suspensions, treated in ultrasonic for 15 min, were centrifuged for 10 min at 2000 rpm. The precipitate at the bottom of the centrifuge tube was removed, and the clear supernatant extract was analyzed for pesticide inhibition by applying the obtained immunosensor detection method.

3. RESULTS AND DISCUSSION

3.1 SEM characterization of the different modified GCE interfaces

SEM was employed to observe the morphologies and microstructures of the modified electrode surface at each immobilization step [33]. As shown in SEM profiles (Fig. 1A), the uniform dispersion GNPs without obvious aggregation could be found. The nanocluster morpha, appeared clearly in the high-magnification image, looks like a pellet with some prickles around it. The SEM image of GS-MB nanocomposite was shown in Fig. 1B. It displayed a regular branched and porous fiber structure. Irregularly sized wrinkled sheet-like structures are observed. Because GS possessed layer structure, from the Fig.1B, we can conclude that the GS had modifed onto the electrode surface successfully. Such nanocomposite film homogeneously on the substrate could provide a conductive pathway of electron-transfer and a favorable microenvironment for immobilization of antibodies.

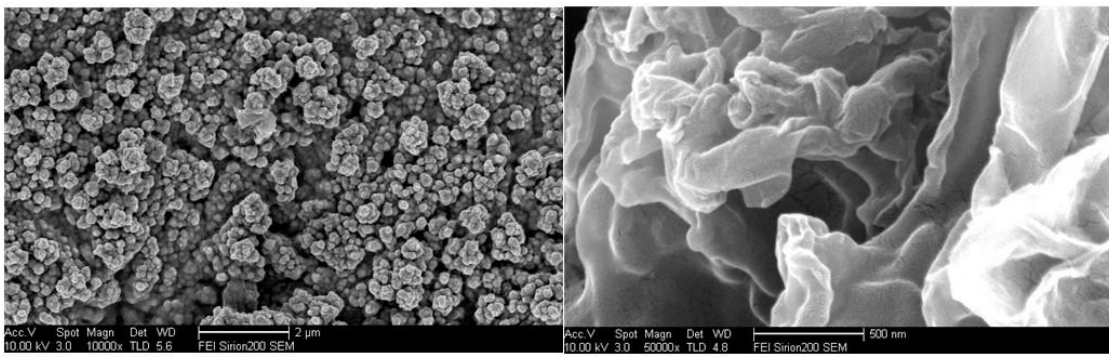

(A) (B)

Figure 1. SEM images of (a) GNPs film; (b) GS-MB film.

3.2 Electrochemical characterization of the modifying process

Fig. 2 showed the CVs of the modifying process in the presence of 0.1 M PBS (pH 7.5) and 5.0 mM $[Fe(CN)_6]^{3-/4-}$ at a scan rate of 50 mV/s. It can be seen that a couple of well-defined redox peaks (Fig. 2a) appeared when the bare GCE was immersed in the detection solution. The peak current increased obviously after DNPs was electrodeposited on the surface of GCE (Fig. 2b), indicated that the GNPs film functioned as an electron-conducting tunnel. When the electrode was coated with GS-MB, the peak current increased again (Fig. 2c), demonstrated that the GS-MB film could promote the electron transfer between electrode surface and $[Fe(CN)_6]^{3-/4-}$. However, after antibody (Fig. 2d) and BSA (Fig. 2e) were absorbed on the electrode surface, the current response was reduced obviously, attributed to their non-electrochemical activity which partially blocked the electron transfer between $[Fe(CN)_6]^{3-/4-}$ solution and the electrode [34]. After chlorpyrifos molecules were combined with the antibodies, a decrease of the redox peaks was observed (Fig. 2f).

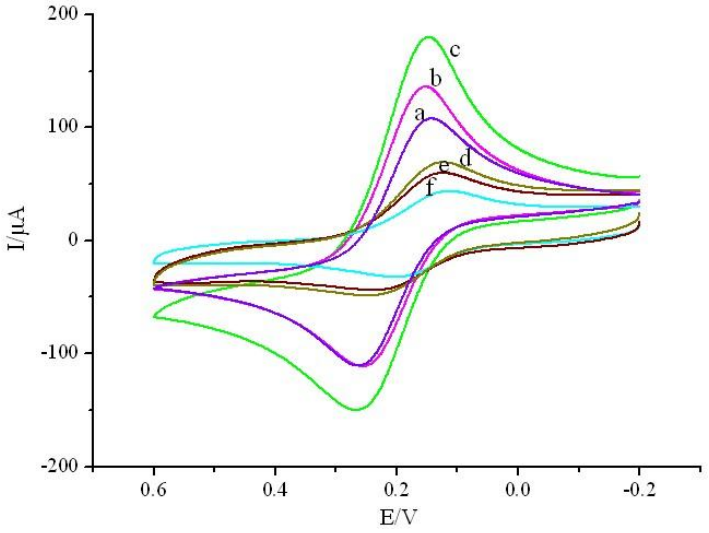

Figure 2. CVs of modified GCE recorded in 0.1 M PBS (pH 7.5) containing 5.0mM $[Fe(CN)_6]^{3-/4-}$ and 0.1M KCl: (a) bare GCE; (b) GNPs/GCE; (c) GS-MB/GNPs/GCE; (d) anti-chlorpyrifos/GS-MB/GNPs/GCE; (e) BSA/anti-chlorpyrifos/GS-MB/GNPs/GCE; (f) chlorpyrifos/BSA/anti-chlorpyrifos/GS-MB/GNPs/GCE.

Fig. 3 illustrated the Nyquist diagram of EIS corresponding to the stepwise modification procedure using $[Fe(CN)_6]^{3-/4-}$ as the redox probe, and the results were in agreement with the conclusions obtained from the CV data.

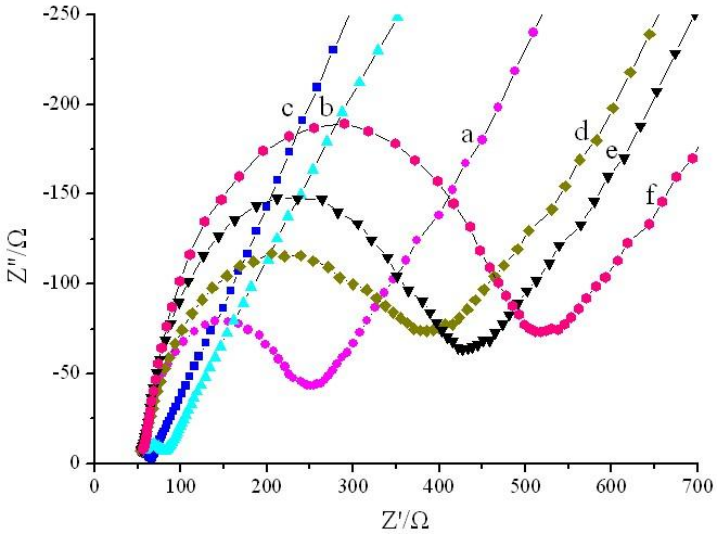

Figure 3. EIS of modified GCE recorded in 0.1 M PBS (pH 7.5) containing 5.0mM $[Fe(CN)_6]^{3-/4-}$ and 0.1M KCl: (a) bare GCE; (b) GNPs/GCE; (c) GS-MB/GNPs/GCE; (d) anti-chlorpyrifos/GS-MB/GNPs/GCE; (e) BSA/anti-chlorpyrifos/GS-MB/GNPs/GCE; (f) chlorpyrifos/BSA/anti-chlorpyrifos/GS-MB/GNPs/GCE.

It can be seen a well defined semicircle at high frequencies and a linear part at low frequencies in the EIS of the bare GCE (Fig. 3a). Compared to the bare GCE, when GNPs (Fig. 3b) and GS-MB

(Fig. 3c) were assembled onto the electrode surface, a significant lower resistance was obtained, implied that the GNPs and GS-MB served as electron conducting materials and accelerated the electron transfer between the electrode and the detection solution. When the electrode was modified with antibody (Fig. 3d) and BSA (Fig. 3e), the Ret increased obviously, attributed to that antibody and BSA acted as inert electron layers and hindered the electron transfer. At last, the Ret increased again in a similar way after the modified electrode was incubated in chlorpyrifos (Fig. 3f), because of the nonconductive properties of biomacromolecule.

3.3 Optimization parameters of the experimental conditions

3.3.1 Influence of the proportion of GS-MB

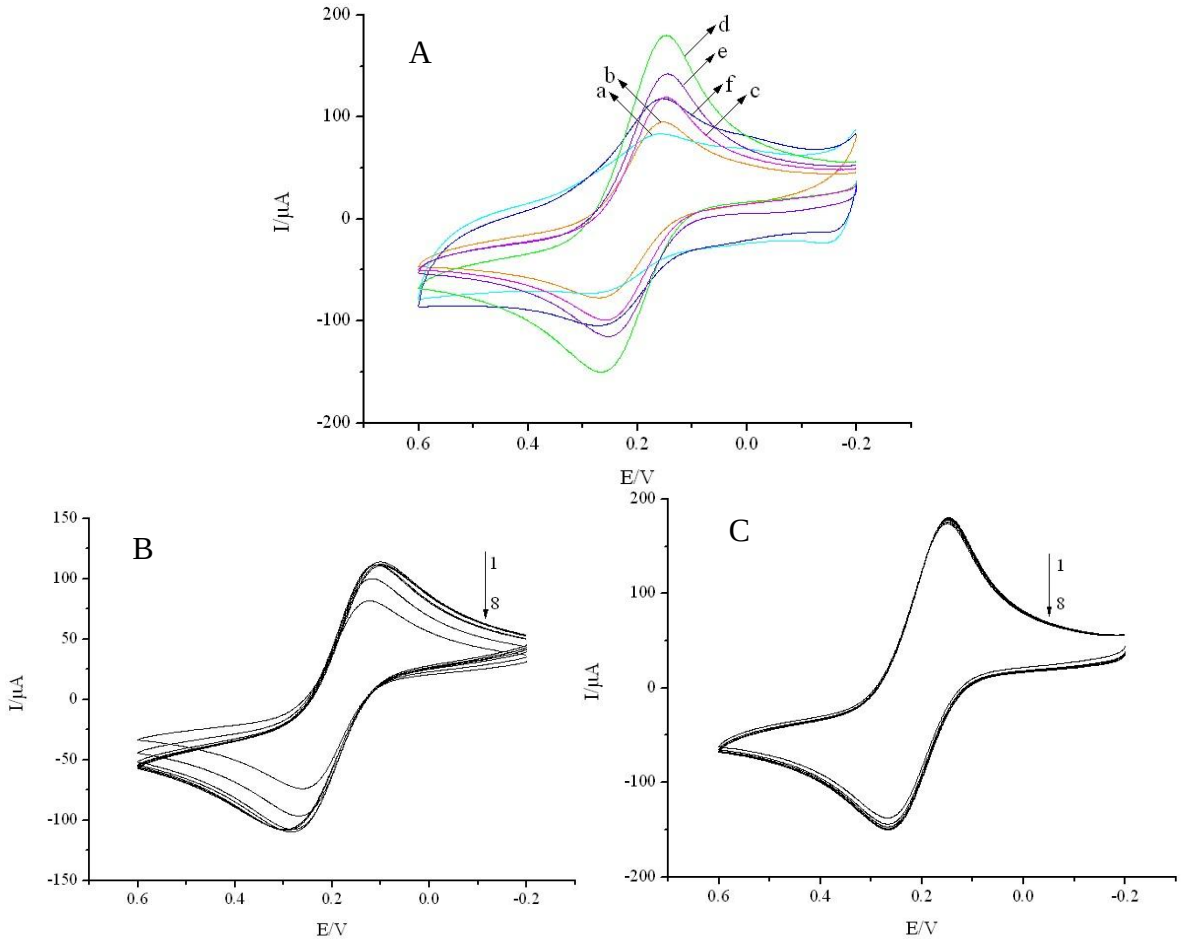

Figure 4. (A) Cyclic voltammograms (CVs) of the GS-MB film-modified GCE: (a) GS:MB=0.5:1, (b) GS:MB=1:1, (c) GS:MB=1.5:1, (d) GS:MB=2:1, (e) GS:MB=2.5:1, (f) GS:MB=3:1. (B) Cyclic voltammograms (CVs) of the GS (without MB); (C) Cyclic voltammograms (CVs) of the GS:MB=2:1.

To receive the optimal proportion of GS-MB, the performances of the electrodes which were coated with different proportions of GS-MB were compared. Firstly, 6 μL of each solution was

dropped onto the surface of the electrode. Subsequently, the CVs of the prepared electrodes were recorded in the detection solution. As shown in Fig. 4A, the current of the electrode modified with the GS-MB mixed in a ratio of 2:1 was higher than others, revealed that the GS-MB proportion of 2:1 amplified the peak current at best. Fig. 4B and Fig. 4C showed the CVs of GS and GS-MB (2:1) -modified electrode scanned 8 circles, respectivelly. As seen, the CVs of GS (without MB)-modified electrode were instable and the current decreased with scanning increase. On the contrary, the CVs of GS-MB-modified electrode were very stable and there were not obvious change in the current with scanning increase. As we all known, the stability of the modified material is of great importance to combine the antibodies and improve the performance of the immunosensor. Therefore, we selected GS:MB=2:1 as the optimal proportion.

3.3.2 Influence of the chlorpyrifos antibody concentration

The specific antibody is an important role on the establishment of the immunosensor [35]. In order to study the effect of the concentration of chlorpyrifos antibody on the performance of the electrode, we investigated the concentration of antibody varying from 1ng/mL to 100 μg/mL. It is clear that the concentration of antibody immobilized onto the electrode should play a key role in the analytical characteristics. As seen in Fig. 5A, the inhibition ratio, that is the relative change in current response, was found to increase with the increasing of the antibody concentration. The inhibition ratio reached the maximum at a concentration of 200 ng/mL. When the concentration was more than 200 ng/mL, the inhibition ratio decreased instead. The main reason is that higher concentration of the antibody the system became saturate and the specific reaction beween chlorpyrifos and anti-chlorpyrifos antibody obeys the mass law. Therefore, 200 ng/mL chlorpyrifos antibody was chosen in further experiments.

3.3.3 Influence of the pH of the detection solution

The pH value of the detection solution is an important factor of the immunosensor performance [36]. The chlorpyrifos antibody modified electrode was incubated in PBS solutions containing 5.0mM $[Fe(CN)_6]^{3-/4-}$ and 0.1M KCl with different pH of 5.0, 5.5, 6.0, 6.5, 7.0, 7.5, 8.0 and 8.5, and the relative changes in current (%ΔI) were measured. The experimental results showed that the inhibition ratio increased with pH value from 5.0 to 7.5, and then decreased when pH value increase again from 7.5 to 8.5 (shown in Fig. 5B). That is to say the the maximum inhibition ratio appeared at pH 7.5. The reasons for that were the biological activity of the antibody as protein declined in acid and alkaline solutions and the antigen-antibody complex could easily be dissociated in the unsuitable pH of working solution. Thus, the detection solution of pH 7.5 was chosen in subsequent experiments.

3.3.4 Influence of incubation temperature

The influence of incubation temperature on the immunosensor response, which has been reported to be vital to the activity of the antibody and chlorpyrifos, was investigated [36]. Fig. 5C

showed the effect of temperature on the current responses at the range from 4 to 50 °C. The inhibition ratio increased as the temperature increased until they reached a maximum value at 37 °C, whereas they decreased when temperatures were over 37 °C. Although 37 °C is the best incubation temperature, high temperature may damage the multilayer film structure and affect the lifetime of the immunosensor. Thus, synthetic consideration for the lifetime, sensivitity of the immunosensor and activity of biomolecules, room temperature (about 26°C) was recommended as the optimal incubation temperature for practical application.

3.3.5 Influence of incubation time

Incubation time is another factor that could influence the response of the immnunosensor, for that a short incubation time would lead to the insufficiency of the reaction and a long incubation time would cause the dissociation of the chlorpyrifos-antibody complex [35]. As displayed in Fig. 5D, the inhibition ratio reached the maximum in 35 min and were stable when the time was extended, indicated that the interaction between antibody and chlorpyrifos had reached saturation. Thus, 35 min was chosen as the optimal incubation time in subsequent experiments.

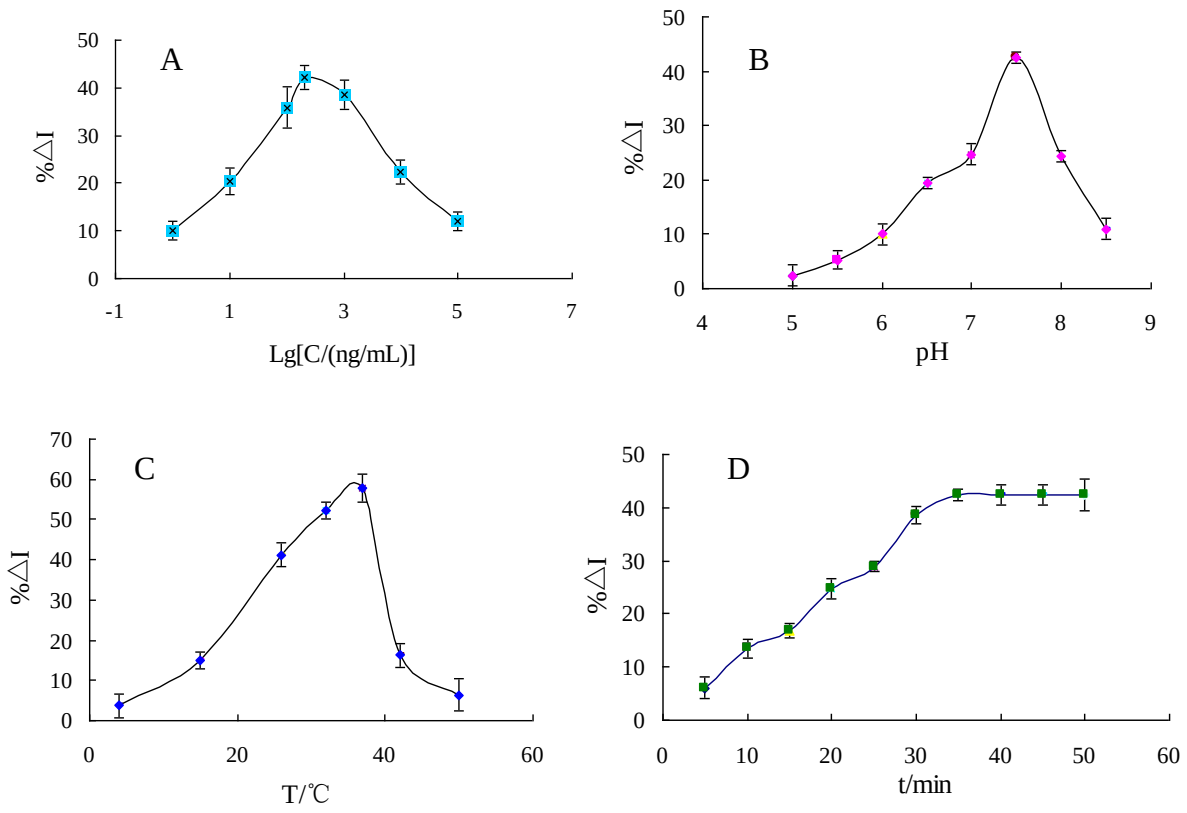

Figure 5. Optimization of experimental parameters: (A) Influence of chlorpyrifos antibody concentration; (B) Influence of detection solution pH; (C) Influence of incubation temperature; (D) Influence of incubation time.

3.4 Calibration curve for chlorpyrifos detection

Under optimal experimental conditions, the calibration plot for detecting chlorpyrifos with the proposed immunosensor is shown in Fig. 6B. It was found that the current response decreased with increasing chlorpyrifos concentrations in Fig. 6A. With more chlorpyrifos binding on the antibodies which was immobilized on the electrode, there would be an additional layer, which come into being a barrier for the electron transfer, thereby a significant decrease in the current response could be observed.

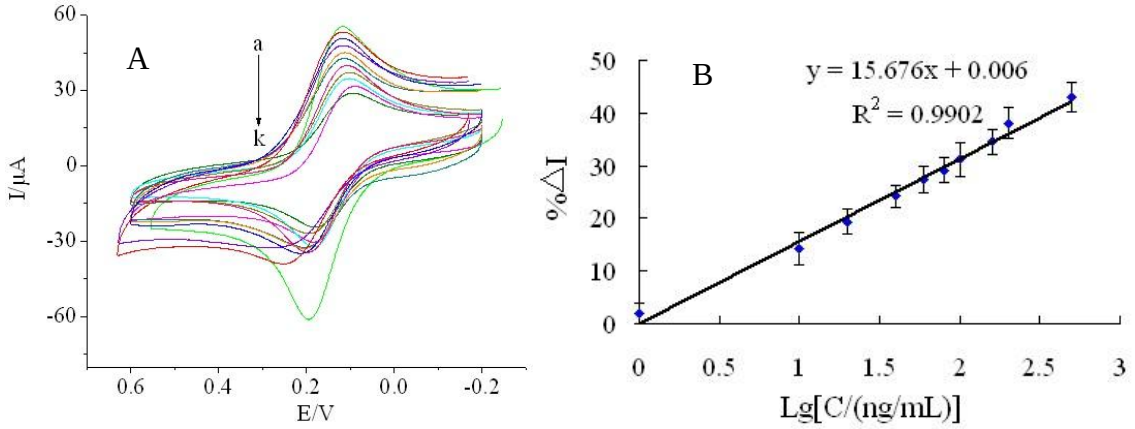

Figure 6. (A) The CVs of the immunosensor after incubation in different concentrations of chlorpyrifos standard solution (from a to k): 0, 1.0, 10.0, 20.0, 40.0, 60.0, 80.0, 100.0, 160.0. 200.0, 500.0 ng/mL under the optimal conditions; (B) The calibration curve of the relative current changes (%ΔI) of the proposed immunosensor versus the logarithm of chlorpyrifos concentration.

Table 1. Comparison of the analytical methods for the detection of chlorpyrifos.

Analytical methods	Liner range (ng/mL)	Detection limit	References
immunochromatography	50-12150	132.91 ng/mL	[37]
β-SPR biosensor system	-	45-64 ng/L	[38]
[BMIM][BF_4]-MWCNT gel-modified CP electrode	3.505-350.5	1.402 ng/mL	[39]
dsCT-DNA/PANI-PVS/ITO	0.5-200	0.5 ng/mL	[40]
AChE/MWCNTs-TCNQ/SPE	0.35-35	0.1 ng/mL	[41]
AChE/CPBA/GR-AuNPs/GCE	0.5-10 10-100	0.1 ng/mL	[42]
BSA/anti-chlorpyrifos/GS-MB/ GNPs/GCE	1-500	0.056 ng/mL	This work

A good linear relationship between the relative current change and logarithm of chlorpyrifos concentration in the range from 1 to 500 ng/mL was obtained in Fig. 6B. The linear regression equation is %ΔI=15.676+0.006lgC (ng/mL) with the correlation coefficients of 0.9902. The detection limit was estimated to be 0.056 ng/mL at a signal/noise of 3 (S/N=3) between the detection signal of low concentration samples and the noise of blank samples. The low detection limit may be attributed to three factors: (1) the GS-MB immobilized on the electrode formed a thin film with relatively high electroactivity; (2) CS, the dispersant which has good biological function and compatibility, can not only enhance the forces acting between the GS-MB film and the GA but also increase the electroactivity of the GS-MB nanocomposite film; (3) GS, with large specific area, could be used to adsorb antibodies and the amount of antibodies conjugated onto GA was greatly improved.

As displayed in Table 1, compared with other reported analytical methods for the detection of chlorpyrifos, the proposed immunosensor had a relative large linear range and lower detection limit, indicating the feasibility and the superiority of the immunosensor which was reliable for the determination of chlorpyrifos.

Compared with the traditional instrumental analytical methods, the proposed immunosensor have some advantages, such as the more shortened sample processing, simplifier sample processing method, and reducing detecting costs, therfore, the proposed immunosensor had great potential for practical application for the analysis of chlorpyrifos in real samples.

3.5 Performance of the immunosensor

3.5.1 Reproducibility and stability of the immunosensor

To evaluate the reproducibility of the immunosensor, a series of five electrodes were prepared for the detection of 200 ng/mL chlorpyrifos. The relative standard deviation (RSD) of the parallel measurements for the five electrodes was 2.8%, confirming that the proposed immunosensor possessed good reproducibility and precision.

Furthermore, the stability of the long-term storage to the modified electrode was evaluated. The prepared immunosensors were suspended over the PBS (pH 7.4) at 4°C for 30 days, and the current responses of the stored immunosensors retained over 86% of their original value, indicating that the obtained immunosensor had an acceptable stability. The good stability could be attributed to the facts that: firstly, the GS-MB nanocomposite possessed good stability and biocompatibility to maintain the bioactivity of the antibodies. Secondly, GA contained two aldehyde groups: one could combine with the amino groups in the chitosan, and the other could connect with the amino groups of chlorpyrifos antibodies leading to firmly immobilize chlorpyrifos antibodies on the electrode.

3.5.2 Selectivity of the immunosensor

To further investigate the selectivity of the proposed immunosensor for chlorpyrifos, the immunosensors were respectively incubated with 200 ng/mL chlorpyrifos coexisting with 200 ng/mL four other interfering substances which present widely in real samples including monocrotophos,

carbaryl, carbofuran, carbofuran-3-hydroxy. No remarkable change of current response was observed in comparison with the result obtained in the presence of interference, indicating good selectivity of the proposed immunosensor.

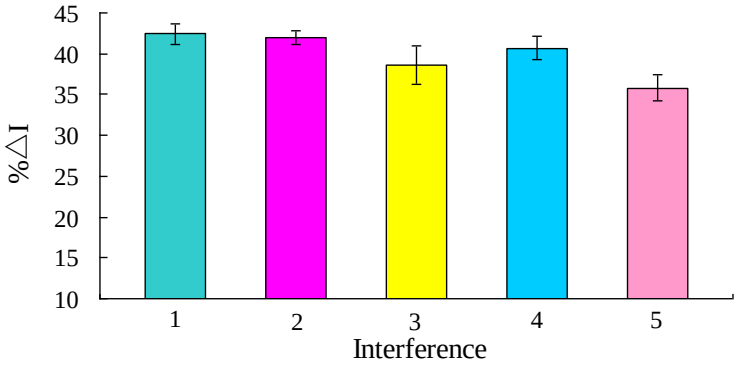

Figure 7. The relative change in peak current (%ΔI) of the proposed immunosensor to: (1) 200 ng/mL chlorpyrifos; (2) 200 ng/mL chlorpyrifos + 200 ng/mL monocrotophos; (3) 200 ng/mL chlorpyrifos + 200 ng/mL carbaryl; (4) 200 ng/mL chlorpyrifos + 200 ng/mL carbofuran; (5) 200 ng/mL chlorpyrifos + 200 ng/mL carbofuran-3-hydroxy.

3.5.3 Regeneration of the immunosensor

A significant factor in the development of a practical immunosensor is the regeneration. After the detection for 200 ng/mL chlorpyrifos, the immunosensor was immersed into the glycine-HCl buffer (pH 2.8) for about 5 min to break the hapten-antibody linkage and washed with PBS solution. As displayed in Fig. 8, the %ΔI gradually decreased with the increase of regeneration times and decreased obviously after regenerating 6 times. The reason may be that anti-chlorpyrifos antibody could gradually shell off or denature and the structure of nanocomposites could be destroyed during continuous being processed by a glycine-HCl buffer and cleaning with the increase of regeneration times. The results demonstrated that the proposed immunosensor could be regenerated and used for at least 6 times.

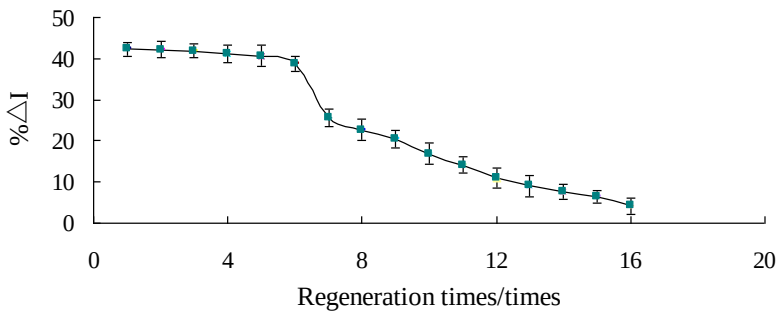

Figure 8. Regeneration performance of the immunosensor.

3.6 Analysis of real samples

In order to investigate the feasibility of the immunosensor for possible applications, the proposed immunosensor was used to determine the recoveries of different concentrations of chlorpyrifos in real samples, including cabbage, pakchoi, lettuce and leek. All the measurements were carried out for three times. The detection value was the average of three results and the analytical results were shown in Table 2. The average recovery was in the range of 86.0%-105.1% which was in acceptable values, and the RSDs between 3.56% and 5.29% were obtained, demonstrating that the proposed immunosensor may provide an efficient tool for chlorpyrifos determination.

Table 2. The recovery of the proposed immunosensor in real samples.

Sample	Added (ng/mL)	Found (ng/mL)	RSD (%) (n=3)	Recovery (%)
cabbage	10	9.76	3.96	97.6
	1.0×10^2	0.93×10^2	4.52	93.0
pakchoi	10	8.84	4.17	88.4
	1.0×10^2	10.37×10^2	3.63	103.7
lettuce	10	10.51	5.29	105.1
	1.0×10^2	0.95×10^2	4.95	95.0
leek	10	9.13	3.56	91.3
	1.0×10^2	0.86×10^2	4.08	86.0

4. CONCLUSIONS

This work developed a novel label-free amperometric immunosensor for the rapid and effective determination of chlorpyrifos residues. The GCE was first modified with GNPs and GS-MB nanocomposite, and GA was subsequently immobilized on the electrode to crosslink with chlorpyrifos antibodies for the detection of chlorpyrifos via an antigen-antibody immune reaction. GS-MB acted as an efficient biointerface film with good biocompatibility can not only enhance the conductivity, but also enlarge the specific surface area of the immunosensor interface, which helped to immobilize antibodies more efficiently. The proposed immunosensor possessed high sensitivity, fast response and good stability, which indicated that not merely it could applied in the laboratory but also it had great potential for practical application for the analysis of chlorpyrifos in real samples.

ACKNOWLEDGEMENTS
This work was supported by the National Natural Science Foundation of China (No.30972055, 31101286), Agricultural Science and Technology Achievements Transformation Fund Projects of the Ministry of Science and Technology of China (No.2011GB2C60020) and Shandong Provincial Natural Science Foundation, China (No.Q2008D03).

References

1. X. Guardino, J. Obiols, M.G. Rosell, A. Farran and C. Serra, *J. Chromatogr. A,* 823 (1998) 91

2. C. Pope, S. Karanth and J. Liu, *Environ.Toxicol. Pharmacol.,* 19 (2005) 433
3. C. Timchalk, J.A. Campbell, G.D. Liu, Y.H. Lin and A.A. Kousba, *Toxicol. Appl. Pharmacol.,* 219 (2007) 217
4. G. Jeanty, Ch. Ghommidh and J.L. Marty, *Anal. Chim. Acta,* 436 (2001) 119
5. Y.A. Kim, E.H. Lee, K.O. Kim, Y.T. Lee, B.D. Hammock and H.S. Lee, *Anal. Chim. Acta,* 693 (2011) 106
6. E. Mauriz, A. Calle, L.M. Lechuga, J. Quintana, A. Montoya and J.J. Mancl´us, *Anal. Chim. Acta,* 561 (2006) 40
7. F.J. Santos and M.T. Galceran, *J. Chromatogr. A,* 1000 (2003) 125
8. C. Blasco, G. Font and Y. Picó, *Food Control,* 17 (2006) 841
9. J. Hernández-Borges, R. Corbella-Tena, M.A. Rodríguez-Delgado, F.J. García-Montelongo and J. Havel, *Chemospher,* 54 (2004) 1059
10. E.P. Syrago-Styliani, G. Evagelos, T. Anthony and A.S. Panayotis, *J. Chromatogr. A,* 1108 (2006) 99
11. O. Eva and S. Manuel, *J. Chromatogr. A,* 1007 (2003) 197
12. P. Bataillard, *TrAC Trends Anal. Chem.,* 12 (1993) 387
13. X.D. Su, S. Low, J. Kwang, H.T. Chew and F.Y. Li, *Analyst,* 125 (2000) 725
14. Y.S. Fung and Y.Y. Wong, *Anal. Chem.,* 73 (2001) 5302
15. Y. Zhuo, R. Yuan, Y.Q. Chai, A.L. Sun, Y. Zhang and J.Z. Yang, *Biomaterials,* 27 (2006) 5420
16. G.D. Liu and Y.H. Lin, *Talanta,* 74 (2007) 308
17. Y.C. Yang, S.W. Dong, T.Shen, C.X. Jian, H.J. Chang, Y. Li and J.X. Zhou, *Electrochim. Acta,* 56 (2011) 6021
18. J.F. Wang, R. Yuan, Y.Q. Chai, S.R. Cao, S. Guan, P. Fu and L.G. Min, *Biochem. Eng. J,* 51 (2010) 95
19. M.H. Yang, S. Sun, Y. Kostov and A. Rasooly, *Lab Chip,* 10 (2010) 1011
20. S. Liu, X.R. Xing, J.H. Yu, W.J. Lian, J. Li, M. Cui and J.D. Huang, *Biosens. Bioelectron.,* 36 (2012) 186
21. D. Du, M.H. Wang, J. Cai, Y.H. Qin and A.D. Zhang, *Sens. Actuat. B Chem,* 143 (2010) 524
22. R. Pauliukaite, M.E. Ghica, O. Fatibello-Filho and C.M.A. Brett, *Electrochim. Acta,* 55 (2010) 6239
23. Y.C. Zhang and C. Ji, *Anal. Chem.,* 82 (2010) 5275
24. K.S. Novoselov, A.K. Geim, S.V. Morozov, D. Jiang, Y. Zhang, S.V. Dubonos, I.V.Grigorieva and A.A. Firsov, *Science,* 306 (2004) 666
25. S. Stankovich, D.A. Dikin, G.H.B. Dommett, K.M. Kohlhaas, E.J. Zimney, E.A.Stach, R.D. Piner, S.B.T. Nguyen and R.S. Ruoff, *Nature,* 442 (2006) 282
26. T.T. Babya, S.S.J. Aravinda, T. Arockiadossa, R.B. Rakhia and S. Ramaprabhu, *Sens. Actuat. B Chem,* 145 (2010) 71
27. K.X. Mao, D. Wu, Y. Li, H.M. Ma, Z.Z. Ni, H.Q. Yu, C.N. Luo, Q. Wei and B. Du, *Anal. Biochem.,* 422 (2012) 22
28. C.S. Shan, H.F. Yang, J.F. Song, D.X. Han, A. Ivaska and L. Niu, *Anal. Chem.,* 81 (2009) 2378
29. C.Q. Ruan, W. Shi, H.R. Jiang, Y.N. Sun, X. Liu, X.Y. Zhang, Z. Sun, L.F. Dai and D.T. Ge, *Sens. Actuat. B Chem,* 177 (2013) 826
30. H. Yao, N. Li, S. Xu, J.Z. Xu, J.J. Zhu and H.Y. Chen, *Biosens. Bioelectron.,* 21 (2005) 372
31. X.H. Lin, P. Wu, W. Chen, Y.F. Zhang and X.H. Xia, *Talanta,* 72 (2007) 468
32. J.L. Wang, F. Wang and S.J. Dong, *J. Electroanal. Chem.,* 626 (2009) 1
33. L. Cui, X.M. Meng, M.R. Xu, K. Shang, S.Y. Ai, Y.P. Liu, *Electrochim. Acta* 56 (2011) 9769
34. J.F. Wang, R. Yuan, Y.Q. Chai, S.R. Cao, S. Guan, P. Fu, L.G. Min, *Biochem. Eng. J.* 51 (2010) 95
35. Ma. Moreno-Guzmán, A. González-Cortés, P. Yá˜nez-Sede˜no, J.M. Pingarrón, *Anal. Chim. Acta* 692 (2011) 125

36. S.T. Jiang, E.H. Hua, M. Liang, B. Liu, G.M. Xie, *Colloids and Surfaces B: Biointerfaces* 101 (2013) 481
37. X.D. Hua, G.L. Qian, J.F. Yang, B.S. Hu, J.Q. Fan, N. Qin, G. Li, Y.Y. Wang and F.Q. Liu, *Biosens. Bioelectron.,* 26 (2010) 189
38. E. Mauriz, A. Calle, L.M. Lechug, J. Quintana , A. Montoya and J.J. Manclus, *Anal. Chim. Acta,* 561 (2006) 40
39. L.G. Zamfir, L. Rotariua and C. Bala, *Biosens. Bioelectron.,* 26 (2011) 3692
40. N. Prabhakar, G. Sumana, K. Arora, H. Singh and B.D. Malhotra, *Electrochim. Acta,* 53 (2008) 4344
41. L. Rotariu, L.G. Zamfir and C. Bala, *Anal. Chim. Acta,* 748 (2012) 81
42. T. Liu, H.C. Su, X.J. Qu, P. Ju, L. Cui and S.Y. Ai, *Sens. Actuat. B Chem,* 160 (2011) 1255